ISBN: 978-3-95450-253-0 ISSN: 2673-5571 doi:10.18429/JACoW-HB2023-TUA1I2

NEW UNDERSTANDING OF LONGITUDINAL BEAM INSTABILITIES AND COMPARISON WITH MEASUREMENTS

I. Karpov*, CERN, Geneva 23, Switzerland

Abstract

Beam instabilities driven by broad- and narrowband impedance sources have been treated separately so far. In this contribution, we present the generalised beam stability analysis based on the concept of van Kampen modes. In the presence of broadband impedance, the loss of Landau damping (LLD) in the longitudinal plane can occur above a certain single-bunch intensity. For significantly higher intensities, the broad-band impedance can drive violent radial or azimuthal mode-coupling instabilities. We have shown that the synchrotron frequency spread due to RF field non-linearity, counter-intuitively, reduces the single-bunch instability threshold. We have also demonstrated that a multi-bunch instability driven by a narrow-band impedance source can be significantly affected by LLD when adding broad-band impedance. These findings are supported by macroparticle simulations and beam observations in the Super Proton Synchrotron and the Large Hadron Collider at CERN.

INTRODUCTION

Interaction of particle beams with the accelerator environment (described in terms of beam-coupling impedance) can lead to beam quality degradation and particle losses. Accelerator performance can be limited by single- or multi-bunch instabilities in the longitudinal plane considered here. Their mechanisms were studied with different approaches [1–24]. Another consequence of beam-impedance interaction could be undamped bunch oscillations observed in different accelerators (Tevatron [25], RHIC [26], SPS [27], and LHC [28]). Usually, they are attributed to the loss of Landau damping (LLD) [1, 2, 4, 6, 7, 29–35], but an alternative theory also exists (soliton solutions of nonlinear equations [26]).

Synchrotron particle oscillations can be described as van Kampen modes [36, 37], which were introduced to accelerator physics in [7]. They represent incoherent synchrotron oscillations as well as undamped or even unstable coherent modes emerged above a certain intensity threshold. The first set of equations to evaluate the stability of bunched beams was proposed in [1]. In general, it has to be solved numerically for a specific stationary longitudinal particle distribution function $\mathscr{F}$ and impedance Z. Under certain assumptions, however, the Lebedev equation [1] allows us to derive the analytical expression for thresholds of coupled-bunch instability (CBI) [10, 38], LLD [35], and generalised multi-bunch instability [39, 40].

A method of solving the linearized Vlasov equation numerically was proposed in [13]. It requires the special ansatz of the perturbed distribution function to convert the Sacherer equation [3] into an eigenvalue problem. This method was originally used for the analysis of single-bunch instabilities in the presence of the potential-well distortion (PWD) revealing a new mechanism of radial mode-coupling instability [13]. Later it was applied to LLD studies [33, 34].

This contribution summarises recent works on LLD [35], single-bunch instabilities in the CERN Super Proton Synchrotron (SPS) [41], and the impact of LLD on multi-bunch beam stability [39, 40].

LOSS OF LANDAU DAMPING

Landau damping of an infinitesimally small perturbation can be understood as the phase mixing of van Kampen modes [7, 33]. Interacting with accelerator impedance, their frequencies are modified as bunch intensity changes. Above a certain threshold, a mode leaves the band of incoherent synchrotron frequencies becoming an undamped coherent mode. This intensity corresponds to the LLD threshold, which is discussed in the following subsection.

Threshold of Loss of Landau Damping

We considered a bunch of particles in a stationary single-RF bucket and dominating inductive impedance above transition energy $\eta \mathrm{Im}Z/k > 0$ (or space charge below transition). The LLD threshold for the dipole mode ($m = 1$) corresponds to a bunch intensity when the coherent frequency, Ω, equals the maximum incoherent frequency of the bunch. According to [35] the LLD threshold in terms of the number of particles in the bunch, N_p, is given by

$$N_{\mathrm{LLD}} = \frac{V_0}{qh\omega_0}\left[\sum_{k=-\infty}^{\infty} G_{kk}(\Omega)\frac{Z_k(\Omega)}{k}\right]^{-1}, \qquad (1)$$

where V_0 is the RF voltage amplitude, q the electrical charge of the particles, h the harmonic number, $f_0 = \omega_0/2\pi$ the revolution frequency, G_{kk} the elements of the beam transfer matrix [42], and $Z_k(\Omega) = Z(k\omega_0 + \Omega)$ the impedance at frequency $k\omega_0 + \Omega$ with $k = \pm 1, \pm 2, ...$

We analysed the binomial family of the stationary distribution function,

$$\mathscr{F}(\mathscr{E}) \propto (1 - \mathscr{E}/\mathscr{E}_{\max})^{\mu}, \qquad (2)$$

with μ defining the bunch shape and $\mathscr{E}$ being the energy of the synchrotron oscillations. The elements G_{kk} at the LLD threshold can be computed analytically by deploying a short bunch approximation (half bunch length in radians $\phi_{\max} \ll \pi$):

$$G_{kk} \approx -i\frac{16\mu(\mu+1)}{\pi\phi_{\max}^4}\left[1 - {}_1F_2\left(\frac{1}{2}; 2, \mu; -y^2\right)\right]. \qquad (3)$$

* ivan.karpov@cern.ch

ISBN: 978-3-95450-253-0 ISSN: 2673-5571 doi:10.18429/JACoW-HB2023-TUA1I2

Table 1: The accelerator and RF parameters of the LHC at injection energy and of the SPS at extraction energy [43].

Parameter	Unit	LHC	SPS
Circumference, C	m	26658.86	6911.55
Harmonic number, h		35640	4620
Transition gamma, $\gamma_{\rm tr}$		55.76	17.95
RF frequency, $f_{\rm RF}$	MHz	400.79	200.39
Beam energy, E_0	TeV	0.45	0.45
RF voltage, V_0	MV	6	7.2

Here ${}_pF_q(a_1,..,a_p;b_1,...,b_q;z)$ is the generalised Hypergeometric function with $y = k\phi_{\rm max}/h$. Since

$$\left|\sum_{k=-\infty}^{\infty} G_{kk}\right| \to \infty,$$

the LLD threshold vanishes for reactive impedance, $Z_k/k = i{\rm Im}Z/k = {\rm const}$, spanning to infinite frequency. The finite LLD threshold requires truncation of the sum at $k_{\rm max}$ and then one obtains

$$N_{\rm LLD} = \frac{V_0\pi\phi_{\rm max}^5}{32qh^2\omega_0\mu(\mu+1)\,\chi(k_{\rm max}\phi_{\rm max}/h,\mu){\rm Im}Z/k}, \quad (4)$$

where we introduced the function

$$\chi(y,\mu) = y\left[1 - {}_2F_3\left(\frac{1}{2},\frac{1}{2};\frac{3}{2},2,\mu;-y^2\right)\right]. \quad (5)$$

For $\mu = 1/2$ and $k_{\rm max}\phi_{\rm max}/h \approx 3.3$, we reproduce LLD threshold according to the Sacherer formalism [23]

$$N_{\rm LLD}^S = \frac{V_0\phi_{\rm max}^5}{18qh^2\omega_0\,{\rm Im}Z/k}. \quad (6)$$

This means that for a given bunch length $\tau_{\rm full} = 2\phi_{\rm max}/\omega_{\rm RF}$ the widely used threshold in Eq. (6) is only accurate for the special choice of the cut-off frequency $f_c = k_{\rm max}f_0 \approx 1/\tau_{\rm full}$. Since the generalised hypergeometric function ${}_2F_3$ approaches zero for $y \to \infty$, the LLD threshold for bunches with $\tau_{\rm full} \gg 1/f_c$ is simplified to

$$N_{\rm LLD} \approx \frac{V_0\pi\phi_{\rm max}^4}{32qh\omega_0\mu(\mu+1)k_{\rm max}{\rm Im}Z/k}. \quad (7)$$

It becomes inversely proportional to the cut-off frequency, and the fifth power in the dependence on the bunch length is replaced by the fourth.

The analytical predictions were confirmed by solving the Lebedev matrix equation semi-analytically as well as using the Oide-Yokoya method [13], also showing that both numerical methods agree (Fig. 1). As expected, there is some discrepancy for larger bunch lengths since the analytic threshold was derived by deploying the short-bunch approximation. The dependence on the cut-off frequency shown in Fig. 2 confirms the vanishing of the LLD threshold for $f_c \to \infty$ [35].

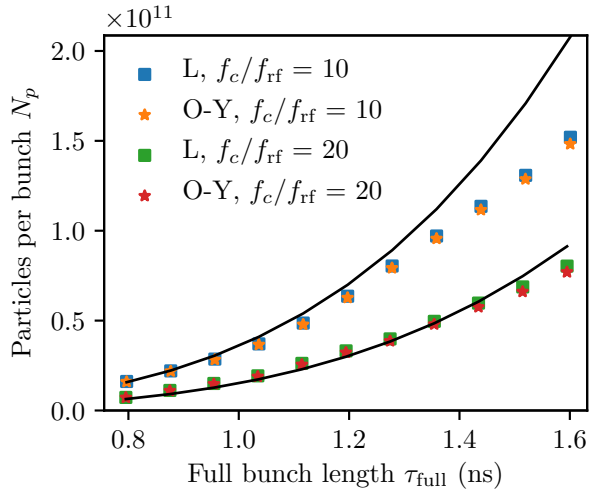

Figure 1: LLD intensity threshold as a function of the full bunch length $\tau_{\rm full}$ calculated using the Lebedev (L) equation and the Oide-Yokoya (O-Y) method for different cut-off frequencies, f_c, of the inductive impedance. The analytic predictions from Eq. (4) are plotted as solid lines. The LHC parameters are according to Table 1, ${\rm Im}Z/k = 0.07$ Ohm, and $\mu = 2$.

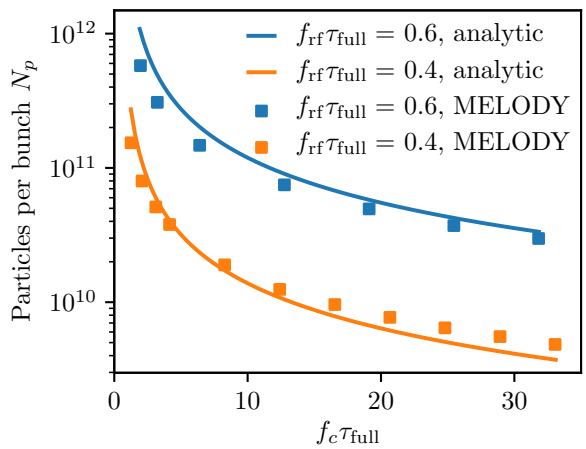

Figure 2: LLD intensity threshold in the logarithmic scale as a function of the cut-off frequency, f_c, of the inductive impedance (multiplied by the full bunch length $\tau_{\rm full}$) for two different values of $\tau_{\rm full}$. The analytic predictions from Eq. (4) are shown as solid lines and the results of semi-analytic calculations using MELODY as squares. Parameters as for Fig. 1.

Effective Impedance

In reality, the impedance could be a complicated function of frequency as it is, for example, the case for the SPS [44, 45]. The form of the LLD threshold in Eq. (1) suggests the definition of the effective inductive impedance

$$({\rm Im}Z/k)_{\rm eff} = \sum_{k=-k_{\rm eff}}^{k_{\rm eff}} G_{kk}{\rm Im}\,(Z_k/k) \Big/ \sum_{k=-k_{\rm eff}}^{k_{\rm eff}} G_{kk}. \quad (8)$$

ISBN: 978-3-95450-253-0 ISSN: 2673-5571 doi:10.18429/JACoW-HB2023-TUA1I2

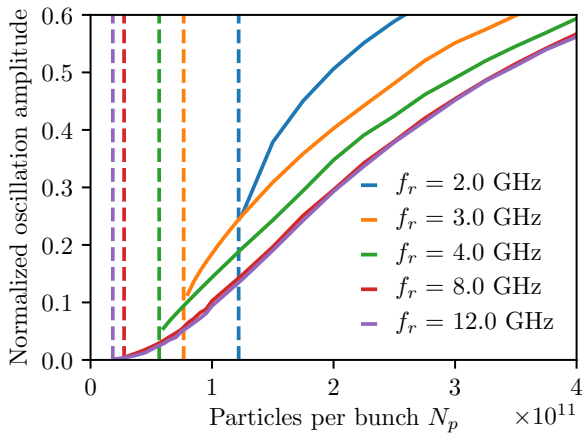

Figure 3: Example of the residual oscillation amplitudes normalised to the initial kick above the LLD threshold versus bunch intensity for different resonator frequencies f_r calculated with MELODY. Dashed vertical lines indicate the corresponding LLD thresholds.

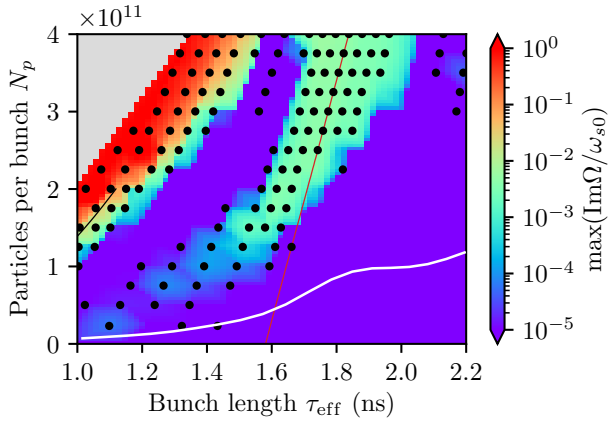

Figure 4: Longitudinal stability map (intensity vs effective bunch length $\tau_{\mathrm{eff}} = \tau_{\mathrm{FWHM}}\sqrt{2/\ln 2}$ scaled from the Full Width Half Maximum (FWHM) value) obtained from calculations with code MELODY. Parameters at the SPS flattop energy with parameters according to Table 1 with $\mu = 1.5$ are used. The colour code shows the growth rate of the most unstable mode, while the grey area indicates parameters for which no stationary distribution was found. The bunch parameters for which the synchrotron frequency is a non-monotonic function of $\mathscr{E}$ are shown as black circles. The black and red lines show examples of the bunch-length dependence on intensity due to PWD for constant energy of synchrotron oscillations $\mathscr{E}_{\max} = 0.12$ and $\mathscr{E}_{\max} = 0.57$, respectively. The LLD threshold is marked as a solid white curve.

The effective cut-off frequency k_{eff} is chosen such that it maximises the cumulative sum in the nominator in Eq. (8) [46]. Thus, the LLD threshold for an arbitrary impedance model can be evaluated by Eqs. (4) or (7) with substitution

$$(\mathrm{Im}Z/k)_{\mathrm{eff}} \to \mathrm{Im}Z/k \text{ and } k_{\mathrm{eff}} \to k_{\max}. \tag{9}$$

This formula was verified for the full SPS impedance as well as for the case of a simple resonator impedance model

$$Z(\omega) = \frac{R}{1 + iQ\left(\omega/\omega_r - \omega_r/\omega\right)} \tag{10}$$

with a shunt impedance R, quality factor Q, and resonant frequency $\omega_r = 2\pi f_r$.

Impact on Beam and Comparisons with Measurements

A beam injected with phase and/or energy error, after a partial initial filamentation, might continue to oscillate if Landau damping is lost. As this initial perturbation is equivalent to a rigid-bunch offset (kick), we studied the long-term bunch evolution by representing the kick as a superposition of van Kampen modes. We see that even though the LLD threshold is lower for higher resonant frequencies, an impact on the beam at the LLD threshold of impedance with higher frequencies is smaller (Fig. 3). As a rigid-dipole perturbation is a common way to study LLD in simulations and measurements, the LLD threshold and residual oscillation amplitude allow us to probe both the effective impedance and its cut-off frequency. This type of measurement, for example, was used recently in the CERN Proton Synchrotron (PS) [47] and SPS [48] to probe their impedance model and study LLD in a double-RF system [49].

The predictions for the case of the LHC assuming $(\mathrm{Im}Z/k)_{\mathrm{eff}} \approx 0.07$ Ohm and $f_r = 5$ GHz (corresponding to the cut-off frequency of the LHC beam pipe [43]) are consistent with observations in measurements [50]. However, the revision of the LHC impedance model at high frequencies is ongoing [51] to have accurate predictions of the LLD threshold for the High-Luminosity LHC (HL-LHC) beam intensity [52].

SINGLE-BUNCH INSTABILITIES IN SPS

The uncontrolled longitudinal emittance blow-up of single proton bunches was observed in the SPS during the acceleration. Due to the strong frequency dependence of the SPS impedance [44, 45], the corresponding instability was mainly studied in macroparticle simulations using the code BLonD [53, 54]. The latest results of simulations through the ramp are very close to beam observations if the latest impedance model is applied as shown in [55].

Depending on the combinations of bunch length and intensity, different types of mode-coupling instabilities are possible [41]. Considering the beam stability at the SPS flattop, the numerical results obtained with the code MELODY (Fig. 4) were able to reproduce non-monotonic dependence of thresholds on intensity. and the presence of the unstable 'island' which were previously observed in simulations [56, 57]. The stability maps at intermediate energies during the acceleration cycle have similar non-monotonic behaviour to

ISBN: 978-3-95450-253-0 ISSN: 2673-5571 doi:10.18429/JACoW-HB2023-TUA1I2

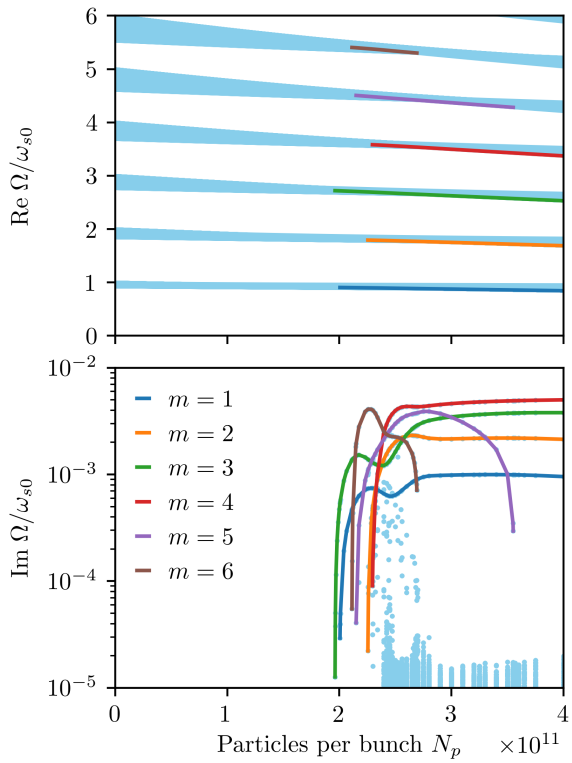

Figure 5: Real (joined by light blue lines, top) and imaginary (blue dots, bottom) parts of van Kampen modes as functions of bunch intensity. The distribution function with $\mathscr{E}_{\max} = 0.57$ corresponds to parameters that belong to the unstable 'island' above the instability threshold. The first six unstable azimuthal modes are plotted as coloured lines. Beam parameters correspond to those indicated for the red line in Fig. 4.

the one at the flat top [58]. We found that the instability in the dedicated measurements corresponds to beam parameters that are inside the unstable 'island' during the part of acceleration.

Radial Mode-coupling Instability

To clarify the instability mechanism inside an unstable 'island' we evaluated van Kampen modes as a function of intensity for constant energy of synchrotron oscillations $\mathscr{E}_{\max} = 0.57$. The real part of the first six azimuthal modes m (Fig. 5, top) does not overlap for the entire intensity range. Thus, the bunch is unstable due to the coupling of radial modes. The lowest threshold intensity is for $m = 3$ (Fig. 5, bottom, green), while for higher intensity other azimuthal modes are also unstable. This can be attributed to 'microwave-like' instability as the bunch line density will be modulated by a mixture of several unstable modes.

Originally, a radial mode-coupling instability was proposed to analyse the stability of very short, electron, bunches, when PWD plays an important role but RF non-linearity can be neglected. Here, the synchrotron frequency distribution

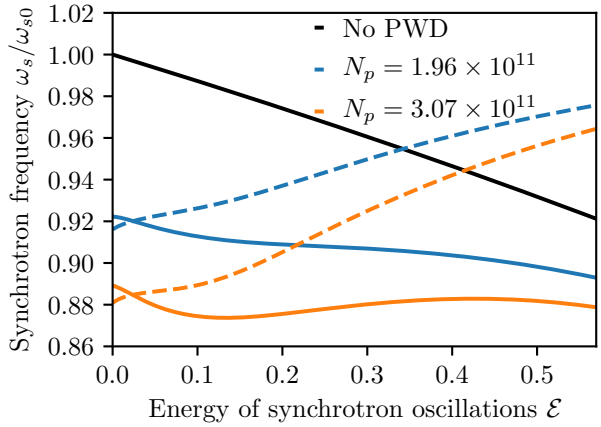

Figure 6: Synchrotron frequency as a function of synchrotron-oscillation energy for different intensities and $\mathscr{E}_{\max} = 0.57$. Solid lines are for single-RF potential, while dashed lines are for a parabolic-RF potential. The black curve illustrates the case without PWD.

ω_s as a function of $\mathscr{E}$ is strongly affected by PWD, and the initial RF non-linearity enhances the non-monotonicity of ω_s (see Fig. 6). At the threshold of instability, (orange) both ω' and ω'' close to zero. For even higher intensities, a more significant overlap of synchrotron frequencies for different $\mathscr{E}$ values is achieved. The instability threshold increases by almost a factor of five if RF non-linearity and PWD are neglected in calculations for $\mathscr{E}_{\max} = 0.57$. It demonstrates the necessity of self-consistent evaluation of the beam stability for relatively long bunches.

Azimuthal Mode-coupling Instability

Another instability type, azimuthal mode-coupling, is also possible in the SPS, but for shorter bunches (Fig. 7). In this case, modes $m = 2$ and $m = 3$ of LLD type (outside the incoherent frequency bands) couple above a certain beam intensity. The threshold obtained in a self-consistent way is slightly lower than the one evaluated neglecting PWD and RF non-linearity. However, the instability is significantly weaker and can be suppressed by a small change in the particle distribution or even an increase of intensity as the modes enter the incoherent frequency band again. For even higher intensity, we also observed a 'mixed' mode-coupling instability, in which the phase-space perturbation involves several azimuthal modes (Fig. 8), and it has higher growth rates (Fig. 7, blue).

MULTI-BUNCH INSTABILITIES

Interaction of particle beams with narrowband (NB) impedance sources can lead to CBI. Its threshold can be evaluated based on the method of stability diagrams [10] derived from the Lebedev equation. However, for most of the existing studies, the contribution of the broadband (BB) impedance was not considered except in a few examples when the CBI growth rates were found in the presence of

ISBN: 978-3-95450-253-0 ISSN: 2673-5571 doi:10.18429/JACoW-HB2023-TUA1I2

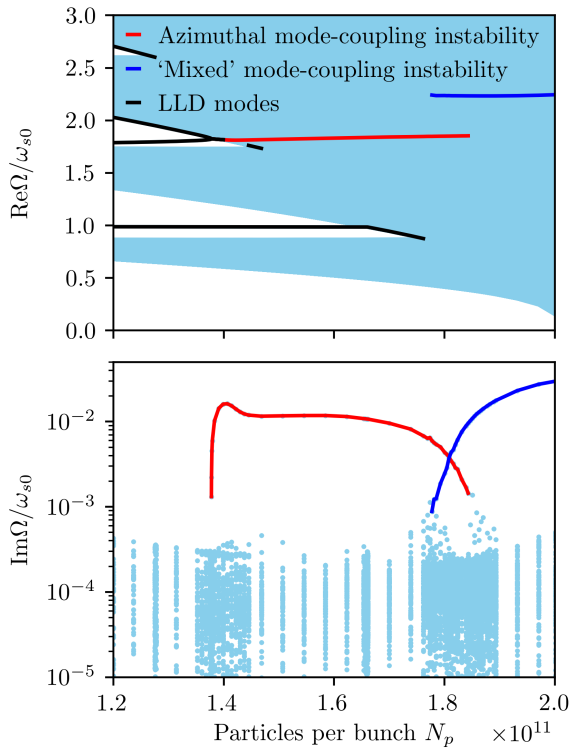

Figure 7: Real (joined by light blue lines, top) and imaginary (blue dots, bottom) as functions of bunch intensity for $\mathscr{E}_{\max} = 0.12$ (bunch parameters correspond to those indicated for the black line in Fig. 4). Black lines show the frequencies of the mode for which Landau damping is lost. The red and blue lines indicate the unstable modes.

two impedance sources [59, 60]. However, the LLD threshold can significantly reduce the CBI threshold [39, 40].

We considered a beam of equidistant M bunches each containing N_p particles. For the case of the narrow-band impedance, with a resonator bandwidth, $\Delta\omega_{\rm nb} = \omega_{r,\rm nb}/2Q_{\rm nb}$, satisfying the criteria

$$\omega_{s0} \ll \Delta\omega_{\rm nb} \ll M\omega_0, \;\; \Delta\omega_{\rm nb} \ll \left|\omega_{r,\rm nb} - \frac{pM\omega_0}{2}\right|, \quad (11)$$

the approximate expression for the CBI threshold can be derived in the short bunch approximation. For the distribution according to Eq. (2), the instability threshold for $\mu > 1$

$$N_{\rm CBI} \approx \frac{V_0\phi_{\max}^4 k_{\rm nb}}{16qh\omega_0 M R_{\rm nb}} \times \min_{y\in[0,1]}\left[\frac{\left(1-y^2\right)^{1-\mu}}{\mu(\mu+1)} J_1^{-2}\left(\frac{yk_{\rm nb}\phi_{\max}}{h}\right)\right], \quad (12)$$

is the lowest for the dipole mode $m = 1$ [38]. Here $k_{\rm nb} = \lfloor\omega_{r,\rm nb}/\omega_0\rceil$, where $\lfloor x\rceil$ denotes the rounding of x to the nearest integer, and $J_m(x)$ is the Bessel function of the first kind and the order m.

To evaluate the instability threshold in the general case when both NB and BB impedance sources are included,

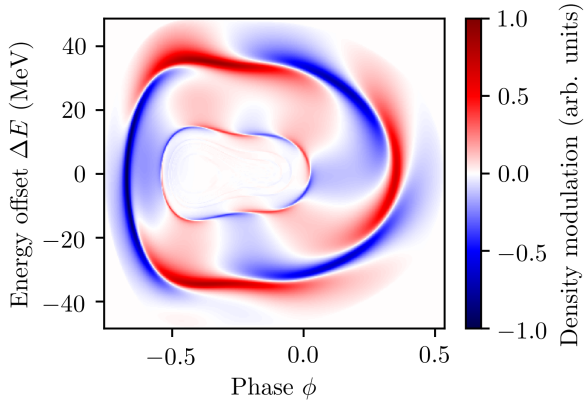

Figure 8: Phase space of the most unstable mode for $N_p = 2.0 \times 10^{11}$ and $\mathscr{E}_{\max} = 0.12$ computed with MELODY using the SPS impedance model from before LS2. The SPS parameters are according to Table 1.

either the Lebedev equation has to be numerically solved or the Oide-Yokoya method needs to be applied. Based on the approach described in [35], we proposed the approximate expression for the generalised instability threshold [39, 40]

$$1/N_g \approx 1/N_{\rm LLD} + 1/N_{\rm CBI}. \quad (13)$$

Here, $N_{\rm CBI}$ and $N_{\rm LLD}$ are defined in Eqs. (4) and (12), respectively. The corresponding unstable coherent mode Ω_g differs from $\Omega_{\rm CBI}$ found for the NB case only, as well as from the LLD case where $\Omega = \omega_s(0)$.

An example of the computed CBI growth rate as a function of the single-bunch intensity for the LHC ring is shown in Fig. 9. The CBI threshold is significantly reduced when the BB impedance is included, compared to the one defined by the higher-order mode (HOM) of Double Quarter Wave (DQW) crab cavities only [61]. Moreover, the instability threshold is very close to the LLD threshold (dashed line) and, thus, dominated by the inductive part of the BB impedance. To make accurate predictions of the CBI threshold for the HL-LHC parameters, the precise BB impedance model is necessary, which is currently under re-evaluation [51].

The final example corresponds to calculations with MELODY for the SPS parameters at extraction energy (Table 1) for different numbers of bunches usually injected into LHC (Fig. 10). The threshold of instability is below the one for LLD and weakly depends on the number of bunches due to a strong impact of the BB impedance in the SPS. For example, for 72 bunches the CBI threshold due to HOMs of 200 MHz RF system around 914 MHz is about 5.5×10^{10}. This is consistent with beam observations where for acceleration of high-intensity LHC beams, an additional 800-MHz RF system is routinely deployed leading to the raised CBI threshold [62]. As expected, above the CBI threshold, the growth rates are larger for a longer train as the instability builds up along the bunches. The results obtained with MELODY

ISBN: 978-3-95450-253-0 ISSN: 2673-5571 doi:10.18429/JACoW-HB2023-TUA1I2

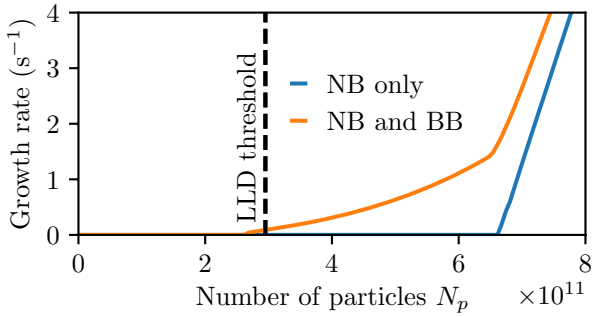

Figure 9: Growth rates of multi-bunch instability versus bunch intensity found with MELODY for the LHC ring with $M = h/10$, $\phi_{\max} = 2.4$, and $\mu = 2$ (see Table 1, except $V_0 = 8$ MV). NB impedance $R_{\mathrm{nb}} = 4 \times 71$ kOhm (four crab cavities), $f_{r,\mathrm{nb}} = 582$ MHz, $Q_{\mathrm{nb}} = 1360$ with and without BB impedance.

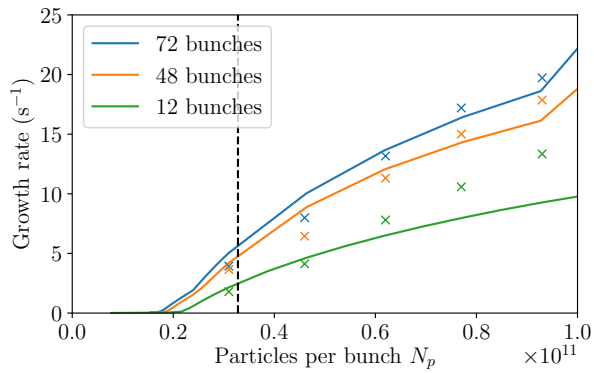

Figure 10: Growth rate of multi-bunch instabilities in the SPS as a function of bunch intensity for different numbers of bunches in the train. The vertical line corresponds to the LLD threshold. The crosses indicate the fitted growth rate from macroparticle simulations with BLonD. Beam and accelerator parameters are from Table 1.

are consistent with the macroparticle simulations using the code BLonD. Some differences can be explained by the fact that several coupled-bunch modes are excited at the same time, which can interfere with and modify the bunch position oscillations.

CONCLUSION

Loss of Landau damping (LLD) and beam instabilities in the longitudinal plane can be important performance limitations for existing and future synchrotrons. The recent studies concerning these effects [35, 39–41] were reviewed in this paper.

The analytic expression for the LLD threshold of the dipole oscillations was proposed for the case of a single RF system and a particle distribution of the binomial family. The threshold is zero for a constant inductive impedance $\mathrm{Im}Z/k$ above transition or capacitive below. Once a finite cut-off frequency is introduced, the threshold becomes inversely proportional to the cut-off frequency f_c once it is larger than the inverse of the full bunch length τ_{full}. The commonly used dependence of the LLD threshold on the bunch length to the fifth power (e.g., based on the Sacherer approach) is justified only for the specific cut-off frequency, $f_c \approx 1/\tau_{\mathrm{full}}$. The dependence of the threshold on the bunch length changes to the power of four for the case of a higher cut-off frequency, $f_c \gg 1/\tau_{\mathrm{full}}$. These studies also led to a new definition of the effective impedance and the corresponding cut-off frequency to estimate the LLD threshold of more complicated impedance models. It is also shown that the impact on the beam close to the LLD threshold is smaller for higher f_c.

Radial and azimuthal mode-coupling mechanisms of longitudinal single-bunch instabilities in the SPS were demonstrated by the self-consistent numerical analysis. The former mechanism, which was typically studied for very short, electron, bunches, is significantly affected by the RF nonlinearity for long proton bunches. For example, the assumption of a linear RF field in the SPS leads to an underestimation of the real instability threshold up to a factor of five. Radial mode-coupling can appear simultaneously for several azimuthal modes for some combination of bunch parameters and thus has a signature of microwave instability. The latter mechanism is also possible in the SPS but for shorter bunches. It is a result of the coupling of the modes that lose Landau damping (moving outside the incoherent frequency bands). It is found that this instability is weaker than the one obtained previously using non-self-consistent analysis. Another instability, 'mixed' mode-coupling, with signatures of both radial and azimuthal mode coupling is possible when there is a significant overlap of synchrotron frequency bands for different azimuthal modes.

Finally, the impact of the broadband impedance on the coupled-bunch instability driven by the narrowband impedance was discussed. A general expression for the multi-bunch instability threshold in the presence of two different types of impedance was proposed. For the considered cases of LHC and the LHC-type beams in the SPS, the instability threshold is significantly reduced when broadband impedance is included in the analysis. It is even lower than the LLD threshold. The new model explains experimental observations and needs to be considered for future synchrotrons.

ACKNOWLEDGEMENTS

I thank Alexey Burov for useful discussions and comments about the loss of Landau damping. I wish to acknowledge Elena Shaposhnikova and Theodoros Argyropoulos for their contributions to our joint work. Special thanks to Alexandre Lasheen, who provided the analyzed data from the dedicated experiments in the SPS. I would like to acknowledge Maxime Gadioux and Sigurd Nese for their excellent work during the CERN Summer Student Programme 2020 and 2021, respectively. I am grateful to Heiko Damerau for his useful comments. Work is supported by the High Luminosity LHC project.

ISBN: 978-3-95450-253-0 ISSN: 2673-5571 doi:10.18429/JACoW-HB2023-TUA1I2

REFERENCES

[1] A. N. Lebedev, "Coherent synchrotron oscillations in the presence of a space charge," *At. Energ.*, vol. 25, no. 2, pp. 851–856, 1968. doi:10.1007/BF01121037

[2] E. Keil and W. Schnell, "Concerning longitudinal stability in the ISR," CERN, Geneva, Switzerland, Rep. CERN-ISR-TH-RF-69-48, 1969.

[3] F. J. Sacherer, "Methods for computing bunched-beam instabilities," CERN, Geneva, Switzerland, Rep. CERN-SI-BR-72-5, 1972.

[4] F. J. Sacherer, "A longitudinal stability criterion for bunched beams," *IEEE Trans. Nucl. Sci.*, vol. 20, no. 3, pp. 825–829, 1973. doi:10.1109/TNS.1973.4327254

[5] F. J. Sacherer, "Bunch lengthening and microwave instability," *IEEE Trans. Nucl. Sci.*, vol. 24, no. 3, pp. 1393–1395, 1977. doi:10.1109/TNS.1977.4328955

[6] G. Besnier, "Stabilité des oscillations longitudinales d'un faisceau groupe se propageant dans une chambre a vide d'impedance reactive," *Nucl. Inst. Meth.*, vol. 164, no. 2, pp. 235–245, 1979. doi:10.1016/0029-554X(79)90241-6

[7] Y. H. Chin, K. Satoh, and K. Yokoya, "Instability of a bunched beam with synchrotron frequency spread," *Part. Accel.*, vol. 13, pp. 45–66, 1983.

[8] J. M. Wang and C. Pellegrini, "On the condition for a single bunch high frequency fast blow-up," in *11th International Conference on High-Energy Accelerators. Experientia Supplementum*. 1980, pp. 554–561. doi:10.1007/978-3-0348-5540-2_72

[9] S. Krinsky and J. M. Wang, "Longitudinal instabilities with a non-harmonic RF potential," *IEEE Trans. Nucl. Sci.*, vol. 30, no. 4, pp. 2492–2494, 1983. doi:10.1109/TNS.1983.4332858

[10] V. I. Balbekov and S. V. Ivanov, "Longitudinal beam instability threshold beam in proton synchrotrons," *At. Energ.*, vol. 60, no. 1, pp. 58–66, 1986. doi:10.1007/BF01129839

[11] J. L. Laclare, "Bunched beam coherent instabilities," CERN, Geneva, Switzerland, Rep. CERN-1987-003-V-1.264, 1987. doi:10.5170/CERN-1987-003-V-1.264

[12] J. P. Garnier, "Instabilités cohérentes dans les accélérateurs circulaires," Ph.D. Thesis, Institut National Polytechnique de Grenoble, Grenoble, France, 1987.

[13] K. Oide and K. Yokoya, "Longitudinal single bunch instability in electron storage rings," KEK, Tsukuba, Japan, Rep. KEK-Preprint-90-10, 1990.

[14] K. Oide, "A mechanism of longitudinal single-bunch instability in storage rings," *Part. Accel.*, vol. 51, pp. 43–52, 1995.

[15] A. Chao, B. Chen, and K. Oide, "A weak microwave instability with potential well distortion and radial mode coupling," in *Proc. PAC'95*, Dallas, TX, USA, 1995, pp. 3040–3042. doi:10.1109/PAC.1995.505777

[16] K. Y. Ng, "Mode-coupling instability and bunch lengthening in proton machines," in *Proc. PAC'95*, Dallas, TX, USA, 1995, pp. 2977–2979. doi:10.1109/PAC.1995.505756

[17] M. D'yachkov and R. Baartman, "Longitudinal single bunch stability," *Part. Accel.*, vol. 50, pp. 105–116, 1995.

[18] A. Mosnier, "Microwave instability in electron storage rings," *Nucl. Instrum. Meth.*, vol. 438, no. 2, pp. 225–245, 1999. doi:10.1016/S0168-9002(99)00832-3

[19] Y. Cai, "Linear theory of microwave instability in electron storage rings," *Phys. Rev. Spec. Top. Accel Beams*, vol. 14, p. 061 002, 6 2011. doi:10.1103/PhysRevSTAB.14.061002

[20] R. R. Lindberg, "Practical theory to compute the microwave instability threshold," in *Nonlinear Dynamics and Collective Effects in Particle Beam Physics*, 2019, pp. 138–146. doi:10.1142/9789813279612_0012

[21] A. Blednykh *et al.*, "New aspects of longitudinal instabilities in electron storage rings," *Sci. Rep.*, vol. 8, no. 1, p. 11 918, 2018. doi:10.1038/s41598-018-30306-y

[22] A. W. Chao, *Physics of collective beam instabilities in high energy accelerators*. New York, NY, USA: Wiley, 1993.

[23] K. Y. Ng, *Physics of Intensity Dependent Beam Instabilities*. Singapore: World Scientific, 2006, pp. 208–212. doi:10.1142/5835

[24] A. W. Chao, M. Tigner, H. Weise, and F. Zimmermann, *Handbook of Accelerator Physics and Engineering*, 3rd ed. Singapore: World Scientific, 2023. doi:10.1142/13229

[25] R. Moore *et al.*, "Longitudinal bunch dynamics in the Tevatron," in *Proc. PAC'03*, Portland, OR, USA, May 2003, pp. 1751–1753. https://jacow.org/p03/papers/TPPB066.pdf

[26] M. Blaskiewicz, J. Wei, A. Luque, and H. Schamel, "Longitudinal solitons in bunched beams," *Phys. Rev. Spec. Top. Accel Beams*, vol. 7, p. 044 402, 4 2004. doi:10.1103/PhysRevSTAB.7.044402

[27] E. N. Shaposhnikova, "Cures for beam instabilities in the CERN SPS and their limitations," in *Proc. HB'06*, Tsukuba, Japan, May-Jun. 2006, pp. 153–155. https://jacow.org/abdwhb06/papers/TUBX05.pdf

[28] E. N. Shaposhnikova *et al.*, "Loss of Landau damping in the LHC," in *Proc. IPAC'11*, San Sebastian, Spain, 2011, pp. 211–213. https://jacow.org/IPAC2011/papers/MOPC057.pdf

[29] V. I. Balbekov and S. V. Ivanov, "The influence of chamber inductance on the threshold of longitudinal bunched beam instability," in *Proc. EPAC'90*, Nice, France, Jun. 1990, pp. 1566–1569.

[30] A. Hofmann and F. Pedersen, "Bunches with local elliptic energy distributions," *IEEE Trans. Nucl. Sci.*, vol. 26, no. 3, pp. 3526–3528, 1979. doi:10.1109/TNS.1979.4330088

[31] O. Boine-Frankenheim and T. Shukla, "Space charge effects in bunches for different rf wave forms," *Phys. Rev. Spec. Top. Accel Beams*, vol. 8, p. 034 201, 3 2005. doi:10.1103/PhysRevSTAB.8.034201

[32] O. Boine-Frankenheim and O. Chorniy, "Stability of coherent synchrotron oscillations with space charge," *Phys. Rev. Spec. Top. Accel Beams*, vol. 10, p. 104 202, 10 2007. doi:10.1103/PhysRevSTAB.10.104202

[33] A. V. Burov, "Van Kampen modes for bunch longitudinal motion," in *Proc. HB'10*, Morschach, Switzerland, Sep.-Oct. 2010, pp. 358–362. https://jacow.org/HB2010/papers/TUO1C03.pdf

ISBN: 978-3-95450-253-0 ISSN: 2673-5571 doi:10.18429/JACoW-HB2023-TUA1I2

[34] A. V. Burov, "Dancing bunches as van Kampen Modes," in *Proc. PAC'11*, New York, NY, USA, 2011, pp. 94–96. https://jacow.org/PAC2011/papers/MOODS4.pdf

[35] I. Karpov, T. Argyropoulos, and E. Shaposhnikova, "Thresholds for loss of landau damping in longitudinal plane," *Phys. Rev. Accel. Beams*, vol. 24, p. 011 002, 1 2021. doi:10.1103/PhysRevAccelBeams.24.011002

[36] N. G. Van Kampen, "On the theory of stationary waves in plasmas," *Physica (Utrecht)*, vol. 21, no. 6, pp. 949–963, 1955. doi:10.1016/S0031-8914(55)93068-8

[37] N. G. Van Kampen, "The dispersion equation for plasma waves," *Physica (Utrecht)*, vol. 23, no. 6, pp. 641–650, 1957. doi:10.1016/S0031-8914(57)93718-7

[38] I. Karpov and E. Shaposhnikova, "Longitudinal coupled-bunch instability evaluation for FCC-hh," in *Proc. IPAC'19*, Melbourne, Australia, 2019, pp. 297–300. doi:10.18429/JACoW-IPAC2019-MOPGW083

[39] I. Karpov and E. Shaposhnikova, "Impact of broadband impedance on longitudinal coupled-bunch instability threshold," in *Proc. IPAC'22*, Bangkok, Thailand, 2022, pp. 2245–2248. doi:10.18429/JACoW-IPAC2022-WEPOMS008

[40] I. Karpov and E. Shaposhnikova, "Generalized threshold of longitudinal multi-bunch instability in synchrotrons", submitted for publication.

[41] I. Karpov, "Longitudinal mode-coupling instabilities of proton bunches in the cern super proton synchrotron," *Phys. Rev. Accel. Beams*, vol. 26, p. 014 401, 1 2023. doi:10.1103/PhysRevAccelBeams.26.014401

[42] E. Shaposhnikova, "Bunched beam transfer matrices in single and double RF systems," CERN, Geneva, Switzerland, Rep. CERN-SL-94-19-RF, 1994.

[43] O. Brüning *et al.*, "LHC design report vol.1: The LHC main ring," CERN, Geneva, Switzerland, CERN Yellow Reports: Monographs CERN-2004-003-V-1, 2004. doi:10.5170/CERN-2004-003-V-1

[44] A. Lasheen and E. Shaposhnikova, "Evaluation of the CERN Super Proton Synchrotron longitudinal impedance from measurements of the quadrupole frequency shift," *Phys. Rev. Accel. Beams*, vol. 20, p. 064 401, 6 2017. doi:10.1103/PhysRevAccelBeams.20.064401

[45] CERN SPS Longitudinal Impedance Model. https://gitlab.cern.ch/longitudinal-impedance/SPS

[46] S. Nese, "Effective impedance for the threshold of loss of Landau damping," CERN, Geneva, Switzerland, Rep. CERN-STUDENTS-Note-2021-214, 2021.

[47] L. Intelisano, H. Damerau, and I. Karpov, "Measurements of longitudinal loss of Landau damping in the CERN Proton Synchrotron," in *Proc. IPAC'23*, Venice, Italy, 2023, pp. 2622–2625. doi:10.18429/jacow-ipac2023-wepa012

[48] L. Intelisano, H. Damerau, and I. Karpov, "Longitudinal loss of Landau damping in the CERN Super Proton Synchrotron at 200 GeV," in *Proc. IPAC'23*, Venice, Italy, 2023, pp. 2626–2629. doi:10.18429/jacow-ipac2023-wepa013

[49] L. Intelisano, H. Damerau, and I. Karpov, "Threshold for loss of longitudinal Landau damping in double harmonic RF systems," in *Proc. HB'21*, Batavia, IL, USA, 2022, paper MOP15, pp. 95–99. doi:10.18429/JACoW-HB2021-MOP15

[50] J. Esteban Muller, "Longitudinal intensity effects in the CERN Large Hadron Collider," Ph.D. Thesis, Ecole Polytechnique, Lausanne, 2016.

[51] M. Zampetakis *et al.*, "Refining the LHC longitudinal impedance model," presented at HB'23, Geneva, Switzerland, Oct. 2023, paper THBP37, this conference.

[52] "High-Luminosity Large Hadron Collider (HL-LHC): Technical design report," I. Béjar Alonso *et al.* (Eds.), CERN, Geneva, Switzerland, CERN Yellow Reports: Monographs, CERN-2020-010, Dec. 2020. doi:10.23731/CYRM-2020-0010

[53] CERN Beam Longitudinal Dynamics code BLonD. http://blond.web.cern.ch

[54] H. Timko *et al.*, Beam longitudinal dynamics simulation studies, Phys. Rev. Accel. Beams, to be published.

[55] J. Repond, "Possible mitigations of longitudinal intensity limitations for HL-LHC beam in the CERN SPS," Ph.D. Thesis, Ecole Politechnique, Lausanne, 2019.

[56] E. Radvilas, "Simulations of single-bunch instability on flat top," CERN, Geneva, Switzerland, Rep. CERN-STUDENTS-Note-2015-048, 2015.

[57] A. S. Lasheen, "Beam measurements of the longitudinal impedance of the cern super proton synchrotron," Ph.D. Thesis, Université Paris Saclay, Paris, 2017.

[58] M. Gadioux, "Evaluation of longitudinal single-bunch stability in the SPS and bunch optimisation for AWAKE," CERN, Geneva, Switzerland, Rep. CERN-STUDENTS-Note-2020-030, 2020.

[59] M. Blaskiewicz, "Longitudinal stability calculations," BNL, Upton, NY, USA, Rep. BNL-81969-2009-IR, 2009.

[60] A. Burov, "Longitudinal modes of bunched beams with weak space charge," *Phys. Rev. Accel. Beams*, vol. 24, p. 064 401, 6 2021. doi:10.1103/PhysRevAccelBeams.24.064401

[61] J. A. Mitchell, G. Burt, R. Calaga, S. Verdú-Andrés, and B. P. Xiao, "DQW HOM coupler design for the HL-LHC," in *Proc. IPAC'18*, Vancouver, BC, Canada, Apr. - May, 2018, pp. 3663–3666. doi:10.18429/JACoW-IPAC2018-THPAL018

[62] "LHC Injectors Upgrade, Technical Design Report, Vol. I: Protons", edited by J. Coupard *et al.*, CERN, Geneva, Switzerland, Rep. CERN-ACC-2014-0337, Dec. 2014.